Journal of Environmental Management 404 (2026) 129415

Contents lists available at ScienceDirect

Journal of Environmental Management

journal homepage: www.elsevier.com/locate/jenvman

Research article

The impact of small-scale variations in floating photovoltaics surface coverage and 'light island' designs on gravel pit thermal structure

Sofia M.G. Rocha [a,*], Regina L.G. Nobre [b], Diego A. Casas [c], Stephen J. Thackeray [d], Alona Armstrong [e], Stéphanie Boulêtreau [b], Julien Cucherousset [b], Andrew Folkard [a]

[a] Lancaster Environment Centre, Lancaster University, Library Avenue, Bailrigg, Lancaster, UK
[b] Centre de Recherche sur la Biodiversité et l'Environnement (CRBE), Université de Toulouse, CNRS, IRD, Toulouse INP, Toulouse, France
[c] Graduate Program of Water Resources and Environmental Engineering, Federal University of Paraná, Curitiba, Brazil
[d] Aquatic Ecosystems Group, UK Centre for Ecology & Hydrology, Library Avenue, Bailrigg, Lancaster, UK
[e] Energy Lancaster, Lancaster University, Library Avenue, Bailrigg, Lancaster, UK

ARTICLE INFO

Keywords:
Photovoltaics
Lake
Hydrodynamics
Renewable energy
Delft3D

ABSTRACT

Photovoltaic energy is projected to represent the largest share of global energy supply by 2050. Floating photovoltaic systems (FPVs) are expected to expand rapidly but their impacts on aquatic ecosystems remain poorly understood. Yet, there is potential for design choices, including the potential for "light island" designs (removing panels across the array to allow for increased light penetration in the water column), to mitigate potential negative effects. Here, we use three-dimensional computational modelling (Delft3D-FLOW), to investigate how the thermal response of a water body is likely to change with multiple light islands designs. The model predicted that the FPVs' effects on the water column temperature vary seasonally and by depth for all designs: wind sheltering effects prevail over shading during warmer months, leading to stronger thermal stratification compared to the simulation without FPVs. Surface coverage variation was the main driver of thermal responses, even for small changes in surface coverage (~5%); light island designs had a limited impact on water temperature and thermal stratification. However, light islands may also impact primary production through enhancement of underwater light availability. Further examination of the effects of light islands on water body biological and chemical responses is required as part of efforts to ensure that FPV deployment strategies balance energy production and sustainable water management.

1. Introduction

Photovoltaics are projected to represent the largest share of global energy supply by 2050 (DNV, 2024). Exponential growth of floating photovoltaic array (FPV) deployment on freshwater bodies - primarily artificial lakes and reservoirs - is widely reported and forecast to grow (Almeida et al., 2022; Liu et al., 2023; Woolway et al., 2024; Xia et al., 2023). FPV have several potential co-benefits, for example they are more efficient than land-based arrays because of the cooling effect of the water (Dörenkämper et al., 2021; El Hammoumi et al., 2021; Sacramento et al., 2015); reduce land use demands of energy installations compared to ground-mounted systems (Nobre et al., 2023); reduce water losses due to evaporation (Kumar and Kumar, 2020; Majumder et al., 2021; Nisar et al., 2022; Santafé et al., 2014); and may mitigate climate change impacts on the host waterbodies (Exley et al., 2021; Liu et al., 2023). Despite this, the physico-chemical and ecological response of hosting water bodies to FPV deployments is poorly understood (Nobre et al., 2023; Ramanan et al., 2024; Rocha et al., 2024).

Given the anticipated growth in FPVs and larger scale deployments, understanding the response of water bodies is critical, especially in small water bodies as they host the majority of existing FPVs (Nobre et al., 2023). Moreover, smaller reservoirs generally have higher FPV relative coverages when expressed as a percentage of waterbody total surface area (Nobre et al., 2024), and thus disturbances to water body physical, chemical and biological processes are likely to be greater. FPVs impact water body processes as they act as a physical barrier to wind mixing and light penetration in the water column (Al-Widyan et al., 2021; Li et al., 2020), with cascading effects on thermal dynamics, biogeochemical cycling and nutrient concentrations, and the abundance and composition of organisms across trophic levels (Li et al., 2023). These physical,

* Corresponding author.
E-mail address: s.midauargondimrocha@lancaster.ac.uk (S.M.G. Rocha).

https://doi.org/10.1016/j.jenvman.2026.129415
Received 6 November 2025; Received in revised form 20 February 2026; Accepted 16 March 2026
Available online 18 March 2026

chemical and biological effects are interlinked in complex ways, and can lead to both positive and negative impacts on water quality and ecosystem health, which may vary spatially and temporally (Dörenkämper et al., 2021; Nobre et al., 2023; Rocha et al., 2024). Understanding the implications of FPVs for water body thermal dynamics is fundamental given the role of temperature in regulating the rates of biological and chemical processes (Brown et al., 2004; Schallenberg et al., 2013).

FPVs generally decrease water temperature due to shading (Exley et al., 2021; Ilgen et al., 2025; Lima Neto, 2025; Nobre et al., 2025). However, in some locations, they have been observed to lead to no temperature difference or even warming. For example, Ilgen et al. (2025) found no significant difference in water temperature in a temperate zone gravel pit lake when 8% of its surface was covered by FPV, and studies of tropical (Yang et al., 2022) and subtropical (Prandini et al., 2025) waterbodies report increased water temperature. These different responses are caused by the effects of varying coverages on the energy balance, including wind mixing and insulating effects (Armstrong et al., 2020; Liu et al., 2024). The percentage coverage will be highly influential on the thermal response given its impact on wind mixing and radiation fluxes (Rueda et al., 2025), but the implications of FPV array geometrical designs are unknown.

There are several ways in which the geometric design of FPV arrays can be altered to modulate water body response. Usually, effects of surface coverage extent have been relatively well investigated, often exploring differences varying more than 10% (Exley et al., 2022; Ilgen et al., 2025, 2023; Ji et al., 2022). For example, Exley et al. (2022) and Ji et al. (2022) applied models, respectively 1D and 2D, to test FPV coverages ranging from 0 to 100% at 10% intervals, while finer changes to coverage are less well understood. A more novel geometric design suggested by industry experts and investigated through a 2D model in Lima Neto (2025), is to create "light islands" which will alter wind mixing and solar radiation receipts in comparison with continuous FPV arrays. Empirical testing of the relative impacts of light island design variants is hampered by experimental design challenges: a Before-After-Control-Impact (BACI) study would require several water bodies with similar characteristics, or there would need to be sufficient time and resource to undertake pre- and post-deployment monitoring of water body state for several different FPVs designs on the same water body, and varying meteorological conditions need to be accounted for. In contrast, computational modelling, which is commonly used to enhance understanding of water body dynamics (e.g., Ishikawa et al., 2022; Zheng et al., 2022; Guo et al., 2023; Xu et al., 2023; Hosseini--Sadabadi et al., 2024), is a rapid and cost effective approach.

To resolve the potential effects of light islands, a 3D modelling approach is necessary, as it allows the incorporation of horizontal transport which is critical when representing light islands effects. Three-D modelling has been found to produce different results from 1D modelling, for example, Ilgen et al. (2025) reported decreased water column stability with every increase in FPV coverage when using a 1D model, whereas a 3D model of the same configuration showed increasing stability for up to 45% coverage (Ilgen et al., 2025). Moreover, 3D models allow resolution of FPV effects across the whole water body, compared to horizontally averaged effects in 1D models.

Given the anticipated growth in FPV deployments and limited knowledge of FPV design variations, this study investigates how the thermal structure of a water body is likely to respond to FPV coverage extent and different light island designs using a 3D model, Delft3D-FLOW (Deltares, 2020). The specific aims were to (1) simulate a water body's thermal response to FPVs deployments that cover different percentages of the host waterbody's surface area, and (2) evaluate how the water body's thermal response varies across a range of light island configurations. Our results provide new insights to guide FPVs design by improving our understanding of the effect of FPV geometric design on the thermal structure of water bodies.

2. Materials and methods

The study was based on a model of a gravel pit lake located in the south of France (latitude: 43.22° N, longitude: 1.61° E, elevation: 245 m a.s.l., Fig. 1). The lake is one of a geographically-clustered group of gravel pit lakes (Gimenez et al., 2023; Zhao et al., 2016), some of which already host FPVs (Nobre et al., 2025). The modelled lake has a surface area of 20.4 ha, a maximum depth of 9.0 m, and a mainly flat bed with steeply sloping sides around its perimeter. Fluctuations in the water level are limited (maximum 13% variation in water depth observed between March 2023 and March 2024), as there are no artificial withdrawals. The main input of water is from precipitation and water table fluctuations.

2.1. In situ data for forcing the model

The model was forced using meteorological and water temperature (September 2022 to March 2024) data measured *in situ*. The meteorological data comprised measurements of air temperature (°C), relative humidity (%), solar radiation (Wm^{-2}), wind speed (ms^{-1}) and direction (degrees) recorded at 10-min intervals at a station immediately adjacent to the lake (Fig. 1 and Figures S1 and S2, data provided by CNR – Compagnie Nationale du Rhône). Additionally, hourly rainfall data were obtained from a Météo-France weather station based in Montaut (latitude: 43.19° N, longitude: 1.64° E, station 9,199,002), approximately 3.5 km from the study site. Water temperature measurements were collected every 10 min using HOBO UA-001-64 temperature loggers (HOBO; Onset, USA) deployed on vertical chains at two sampling locations in the lake (Fig. 1) at multiple depths, starting at 0.5 m then 1.0 m and every metre to the lake's bed, totalling eight points (details in Nobre et al., 2025).

2.2. Modelling methodology

2.2.1. Delft3D-FLOW set-up

Delft3D-FLOW is used here as a three dimensional hydrodynamic and transport simulation model that reproduces non-steady flow and transport phenomena resulting from meteorological forcing using a curvilinear grid structure (Deltares, 2020). Simulation time is dependent on the availability of forcing data at a sufficiently fine sampling interval. In this case, these data were fully available from September 2022 to March 2024 at every 10-min, and initial conditions for water level and temperature measured on September 9th' 2022 were used. The modelled reservoir was approximated by a uniform curvilinear grid with 60 points in M-direction (horizontal equivalent) and 50 points in N-direction (vertical equivalent), resulting in squared cells of around 10 m. The simulation time step was 0.02 min. Forcing input data consisted of air temperature (°C), relative humidity (%), solar radiation (Wm^{-2}), cloud cover (%), wind speed (ms^{-1}) and direction (degrees), and rainfall (mm).

Sensitivity tests were conducted using temperature data collected between September 2022 and February 2023 to determine how the model results respond to variations in multiple parameters that dictate physical processes in the lake (see SI). The sensitivity analysis was restricted to autumn and winter given this was the only period for which consistent forcing and validation data were available at the time. Despite the lower irradiance, this period captures a broad range of hydrodynamic conditions, and the good calibration and validation performance indicates that the dominant system dynamics were adequately represented. Calibration and validation of the model were performed by varying the values of parameters related to heat and momentum transfer at the surface and heat transport in the water column, informed by the sensitivity tests. Specifically, these parameters comprised the Secchi depth, Stanton number, background eddy viscosity and diffusivity for both vertical and horizontal directions, which were varied within ranges of possible values informed by the sensitivity tests and previous studies

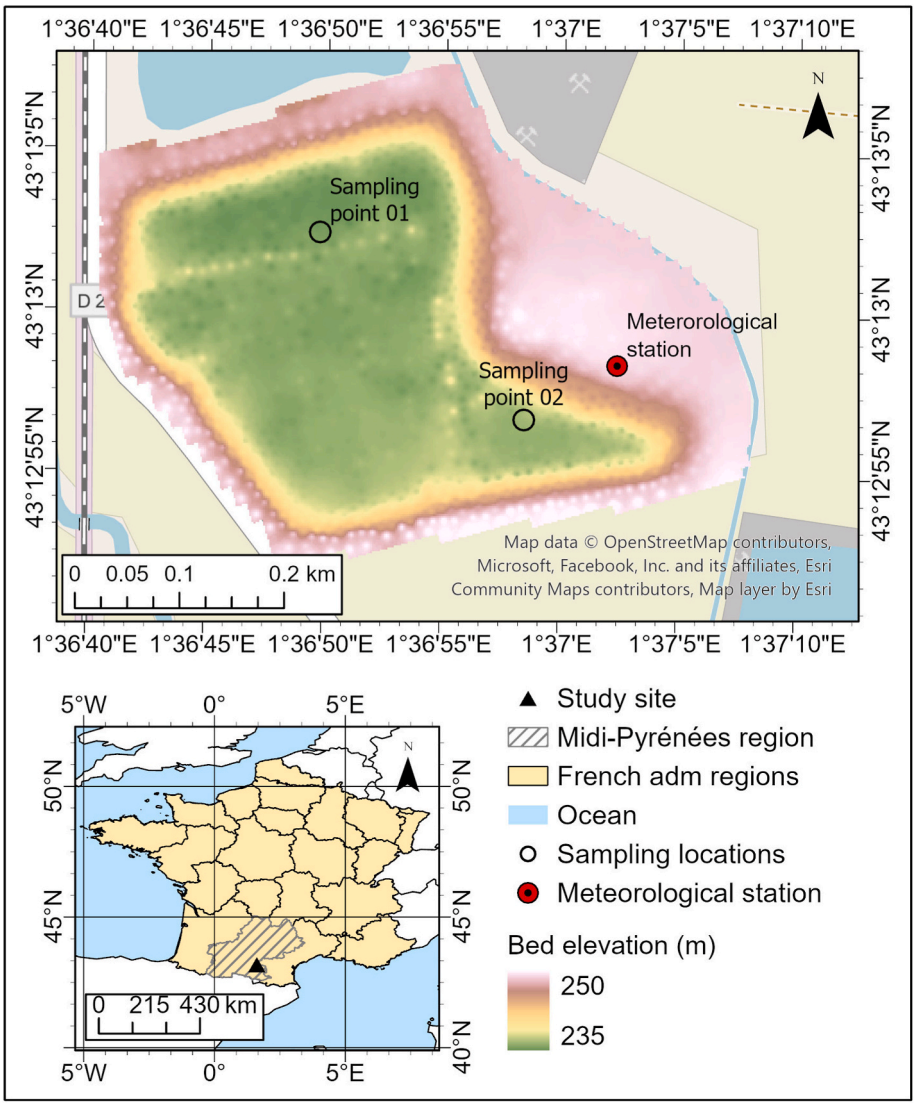

Fig. 1. Study site schematic location. Bathymetric data provided by CNR.

(Amadori et al., 2021; Ishikawa et al., 2022; Rocha et al., 2023). At these stages, no FPV coverage was simulated in the model.

Calibration and validation were carried out using half of the forcing datasets each. Model performance was assessed by comparing *in situ* measured and modelled vertically averaged water temperature (T_{mean} [°C]), and potential energy anomaly (φ [Jm^{-3}]). The latter is a quantification of the strength of the water column's thermal stratification and is defined as

$$\varphi = \frac{1}{H}\int_{-h}^{\eta} [\underline{\rho} - \rho(z)] g z dz \quad (1)$$

where ρ (z) is density [kg/m^3] at depth z, $H = \eta + h$ is the water column depth [m], $z = \eta$ the height of the free surface [m], $z = -h$ is the depth of the bed [m], $\underline{\rho}$ is the depth-averaged density [kg/m^3], g is the gravitational acceleration [m/s^2], and z is the vertical coordinate [m], which is measured positive upwards from the water surface, which is set at z = 0.

Model output was saved every 6 h of simulated time and then compared to the corresponding (time-matched) *in situ* measurements. Three metrics were used to evaluate model performance: coefficient of determination, r^2, root mean square error, RMSE, and mean error, or bias (see SI for equations) capturing both the model's relative fit and its absolute accuracy, while also assessing and minimizing any systematic bias. Both calibration and validation were performed by analysing data for the two sampling locations in the lake. All data analysis was developed using the Python v.3.11.4 (Python Software Foundation, 2023).

The values of r^2, RMSE, and bias for T_{mean} and φ at each of the two measurement locations for the calibration and validation periods are shown in Table S1. The calibrated values of the adjusted model parameters are shown in Table S2, and are all within the range of values reported from similar previous studies (Amadori et al., 2021; Ishikawa et al., 2022; Piccioni et al., 2021; Rocha et al., 2023; Xu et al., 2017).

2.2.2. Model representation of FPVs

Representation of the FPV coverage within the model was achieved by applying attenuation factors α to the incoming solar radiation and wind speed at the hydrodynamic grid cells where the structures were allocated. Thus, the magnitude of the meteorological variable at the water surface beneath the FPV was calculated as $X_{FPV} = (\alpha)X_{open}$, where X_{open} is the corresponding value in open water, similarly to Exley et al. (2021). The magnitude and spatial distribution of FPV-induced effects depend on array technology, for example whether the panels have fixed-tilt or tracking systems, their distribution on the surface and the float design. These characteristics affect shading patterns, wind sheltering, and heat exchange. In this study, we focus on a fixed-tilt

configuration as it represents the most widely deployed FPV technology, particularly in reservoir applications. We represented the design of FPV array generally observed in the study area (Nobre et al., 2025), i.e. with photovoltaic panels mounted on rectangular, buoyant plastic platforms. The system used a modular layout that allowed sunlight to pass between the panels and reach the water surface.

Previous efforts to determine FPVs' effects on meteorological forcing of lakes that used *in situ* data have found wide variations in their attenuation factors. Values of $\alpha = 0.23$ to 1.00 for wind speed and $\alpha =$ 0.73 to 0.88 for solar radiation have been reported (Ilgen et al., 2023, 2025; Liu et al., 2024; Yang et al., 2022). Solar radiation attenuation has also been observed to be dependent on meteorological conditions. For example, during rainy periods, attenuation of solar radiation by FPVs is weakened or eliminated (Liu et al., 2024). Therefore, even though empirical data exist for meteorological forcing reduction due to solar panels, their implications are not reliably transferable among sites or applicable to models. Here, we investigate changes to solar radiation and wind speed assuming a 1:1 relationship between the two, e.g., if the incoming solar radiation is attenuated through a factor of 0.4, this same factor is applied to the wind speed reaching the water surface. This conservative assumption is justified given the wide range of variability of these factors in the literature (no measurements are available for solar radiation or wind speed under the FPV array).

In this study, we were able to access empirical data recorded through a BACI study in a set of gravel pit lakes similar in bathymetry (though somewhat shallower - mean depth approximately 5 m) and nearby to our study site (Nobre et al., 2025), and we used these to calibrate the attenuation effects of the FPVs in the model. Specifically, Nobre et al. (2025) conducted a BACI study in six gravel pit lakes: three lakes with FPVs compared to three non-FPVs lakes, resulting in three paired lakes. The three lakes with FPVs had, on average, 49.1% coverage (SD = 7.9%), and this was the coverage defined in the model for our study site. The depth-averaged water temperature for the three non-FPVs lakes from Nobre et al. (2025) was compared to that from the top 5 m and the full depth for this study site (Fig. S3). This showed that the top 5 m average for this study site follows a similar pattern to that of Nobre et al. (2025). Therefore, the averaged water temperature for the top 5 m ($T_{mean\ 5m}$) of this study site was compared to the BACI results from Nobre et al. (2025) to assess the model representation of FPVs.

Both solar radiation and wind speed were assumed to be equally affected at the FPV site on the water surface and were therefore scaled using the same attenuation factor, similar to Bredeweg et al. (2025). To test this, six values of α (ranging from 0.45 to 0.70 in steps of 0.05) were simulated. For each simulation, we calculated the difference in mean water temperature over the upper 5 m ($\Delta T_{mean\ 5m}$) between two cases: (1) a point beneath the FPVs in the FPV-covered model, and (2) the same location in the model without FPVs. To identify the most accurate α value, we evaluated model performance using r^2, Root Mean Square Error (RMSE), and bias (Table 1). These metrics allowed comparison of the modelled temperature differences between FPV and non-FPV scenarios with observed differences from the BACI study (Nobre et al., 2025). In that study, observations were averaged across three paired lakes, and all values represent the mean temperature over the upper 5 m of the water column.

Table 1
Comparison of modelled and observed FPVs-induced water temperature changes (0–5 m mean) for the period with available data, between October 09, 2022 and December 10, 2023.

α Factor	r^2	RMSE (°C)	Bias (°C)
0.45	0.73	0.93	0.79
0.50	0.72	0.77	0.58
0.55	0.72	0.64	0.39
0.60	0.73	0.56	0.23
0.65	**0.71**	**0.56**	**0.02**
0.70	0.68	0.63	−0.18

This calibration determined that an attenuation factor of 0.65 (Table 1), for both wind speed and solar radiation, resulted in the closest match between measured and simulated water temperature differences due to FPV coverage. There is greatest deviation between the modelled and measured $\Delta T_{mean\ 5m}$ data during the winter period between November 2022 and February 2023 when FPV effects on $T_{mean\ 5m}$ are smallest (<1 °C) and the model slightly overestimates them (Fig. S4). From thereon, the model data follow the average measured temperature differences closely, despite not capturing some short timescale (<1 month) variations. The fact that the calibrated model captures higher FPV impacts over spring, summer and autumn, when ecological activity is likely to be highest and water quality impacts are likely to be greatest, gives us confidence in its suitability for representing FPV impacts through the attenuation of meteorological forcing.

2.2.3. Model outputs

We investigated the variation in FPV effects on the thermal stratification and averaged water column temperature of the study site over time and space. Initially, a surface coverage of 46% was modelled, following the average coverage in the region (Nobre et al., 2025), respecting a 40 m distance from the shore, and applying the α factor calibrated in 2.2.2. This standard array configuration has continuous cover, i.e., without any light islands. The model results for the uncovered lake were compared to the model run with 46% coverage for a point location in the middle of the lake to define a baseline for the assessment of array configurations incorporating light islands. Here, the analysis for a point location was defined to be consistent with existing literature (Ilgen et al., 2025; Nobre et al., 2025; Prandini et al., 2025; Yang et al., 2022). We analysed the following indicators of waterbody physical structure: water temperature at multiple depths, T_{mean} and φ.

2.2.4. FPVs array configuration scenarios

Following simulations of the reservoir's thermal response to an FPV array with a continuous cover, eleven scenarios were developed. They varied in both the overall percentage of light islands as well as the light island size, while keeping the same global FPV array perimeter in the centre of the reservoir. The percentage of FPV cover varied from 37% to 46%, as typical in the region on gravel pit lakes. 46% coverage was set as the base case (Fig. 2a), without light islands. The FPV array was at least 40 m from the shore as this is required by French regulation to avoid effects on the littoral zone. Variations around the maximum coverage were defined based on the implementation of light islands, i.e., how much the coverage would reduce to accommodate light islands. The resulting scenarios included continuous surface coverages of 37%, 41%, 43%, and 46% (Fig. 2a to d). Simulations were conducted with light islands covering 20%, 10%, and 5% of the array area (Fig. 2e to g) and variations in the light island gap resolution while maintaining a similar overall surface coverage (41%) and 10% of gaps (Fig. 2h to k).

We investigated how the reservoir's response to the different FPV designs varied by comparing simulated water body thermal responses among them. This was achieved by initially analysing heatmaps of the water temperature at the surface of the lake, followed by comparing the horizontally averaged effect of the array on T_{mean} among scenarios. The heatmaps were plotted for the day and time with the largest difference in water temperature between the simulations with and without FPV coverage, i.e., August 7, 2023 at 6 a.m. This conservative choice assumes that the day with the largest difference best captures spatial variability, since analysing heatmaps for the entire time series was impractical. Subsequently, time series for T_{mean} were compared between each scenario and the baseline simulation without FPV coverage, where negative values represent cooler water in the covered scenario. At this stage, an averaged effect was investigated rather than a point location to capture effects of the FPV on the water column using 3D modelling outputs.

Multiple horizontal aggregation methods were applied to calculate the average impact on the water temperature, including: (1) only cells with FPV coverage, (2) all cells enclosed by the array perimeter, and (3)

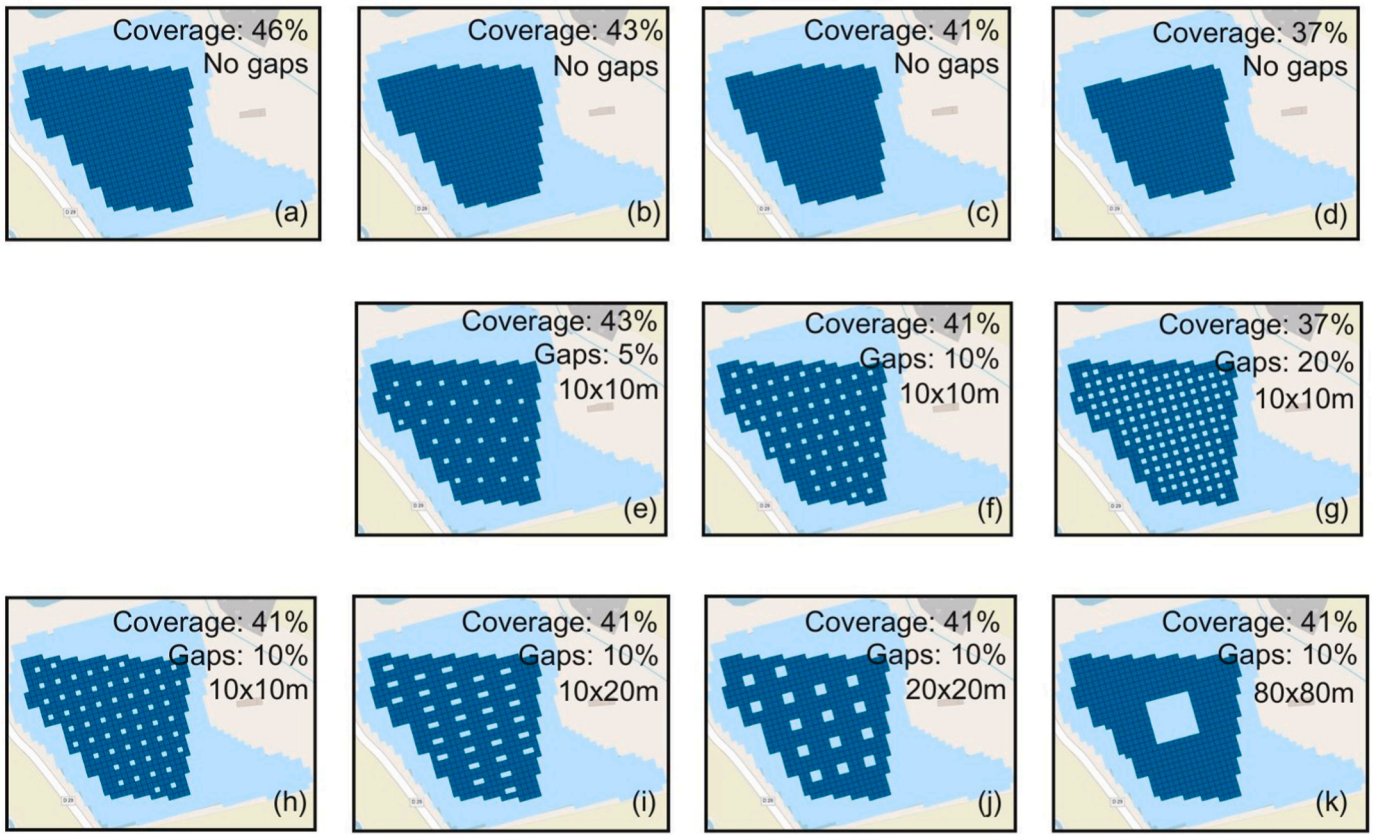

Fig. 2. Illustration of the modelled FPVs scenarios in the studied lake. The FPV coverages in (b), (c) and (d) correspond to the coverage after removing the cumulative surface of light islands in (e), (f) and (g), respectively.

the whole surface of the lake (SI Figure S5). Preliminary analysis indicated that the quantified impacts of FPVs on water temperature did not differ among these approaches (Fig. S6), and so further analysis of water temperature in this study includes only impacts averaged under the FPVs. The responses of φ were also investigated. Since the model calculated values of φ for every grid cell in the 3D model, its maximum value in the lake was chosen as representative of the strength of the lake's thermal stratification.

3. Results

3.1. FPV coverage impacts on lake thermal response

The temperature of the open water point (Fig. 3a) was consistently cooler with the FPVs in place (Fig. 3b), with an average decrease of 1.51 °C over the simulated year 2023. A clear seasonal trend was observed, characterised by a larger impact during the warmer months: between April and August 2023 the depth-averaged water temperature was cooler than that without FPVs by 2.20 °C, whilst between October 2022 and January 2023, a 0.96 °C cooling was observed.

Notably, the magnitude of cooling differed between the surface and bottom layers (Fig. 3c). The yearly average (based on 2023) cooling of the modelled water temperature at 0.5 m was 1.28 °C, while at 7.0 m deep the decrease was 1.90 °C. However, the trend varied during the year, with surface waters experiencing a larger cooling effect (1.31 °C) due to the FPV compared to the bottom layers (0.53 °C) in February (Fig. 3c), which then reversed as air temperature increased, and summer started. Consequently, in June, the average cooling effect of the FPV was 1.39 °C at a 0.5 m depth and 3.10 °C at 7.0 m, resulting in a relatively cooler hypolimnion compared to the epilimnion.

Stronger thermal stratification (higher φ), was found in the simulations with the FPV between April and August, when thermal stratification was established (Fig. 3d), resulting from the increasing vertical temperature gradient beneath the FPVs (caused by stronger cooling in deeper water). The difference in stratification strength with FPV compared to that without varied between months. For example, in April 2023 and August 2023 (respectively the start and end of higher solar radiation period) the estimated φ with and without FPV coverage was, respectively, 6.06 and 5.03 J/m^3 (simulation with FPV showed a 20% stronger stratification compared to the simulation without FPV) whilst in June 2023 (peak solar radiation) (see SI Figure S1), the estimated φ was only 6 % larger (18.70 J/m^3) than that without FPV coverage (17.60 J/m^3). Further, in August the estimated φ with FPVs (10.77 J/m^3) was 59% higher than that without (6.79 J/m^3), when remarkably lower values were noted.

3.2. Influence of "light island" configuration

There was no horizontal spatial heterogeneity in surface water temperature (Fig. 4), i.e., the changes to water temperature observed away from the array were similar to those under it. The principal driver of surface water temperature was the surface coverage rather than the light island configuration: similar surface water temperature was observed for the scenarios with the same FPV coverages (Fig. 4b and e), with cooler temperatures observed for higher FPV coverages (Fig. 4a to d). Similarly, no difference was observed for varying light island designs (Fig. 4h to k).

Temporal water temperature responses between the FPV coverage scenarios were also predominantly driven by changes in the surface coverage (Fig. 5). The yearly average (for 2023) decrease in temperature was approximately 1.80 °C for the 43% coverage for both the continuous array and the scenario with 5% of gaps. Meanwhile, the 41% coverage scenarios showed an average decrease of ~1.70 °C and the 37% coverage scenarios a decrease of ~1.50 °C. The averaged water

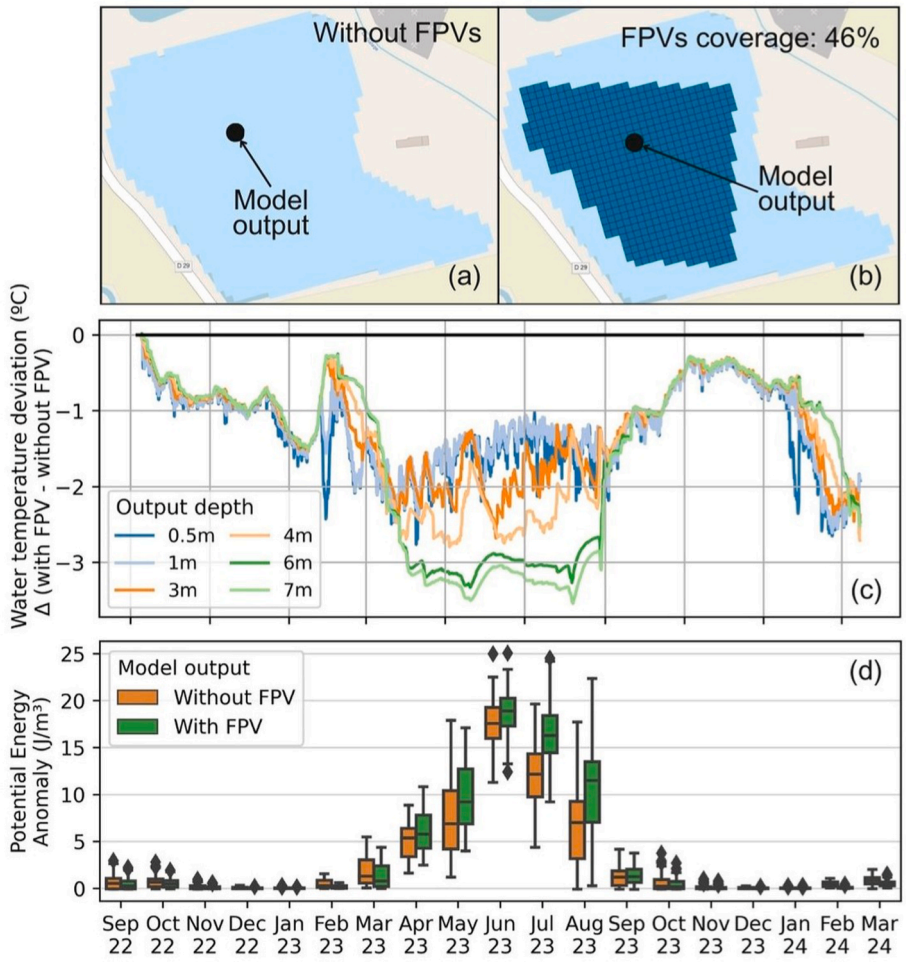

Fig. 3. Model output locations (a) without and (b) with FPVs, (c) horizontally averaged water temperature differences at different depths and (d) Potential Energy Anomaly (φ) between the simulations with and without FPVs over time for a point location in the lake. At the start of the simulation, a spin-up period is observed, where the temperature with the FPVs is the same as that without FPVs ($\Delta = 0$). In October 2022, the temperature difference stabilises, and this is when the model starts to accurately reproduce the FPVs' coverage.

temperature impact difference among the scenarios was larger in the warmer months, i.e., April, May, June, and July. Specifically, for the 43%, 41% and 37% coverages, ~3.05 °C, ~2.90 °C and ~2.60 °C cooling was observed compared to the simulation without FPVs, respectively.

Thermal stratification (Fig. 6) was similar between the light island scenarios. Importantly, the stratification duration was similar, with higher φ between April and August. Specifically, the mean φ between April and August was 9.73 J/m^3 for the run with 46% coverage of FPVs and 7.68 J/m^3 for the run without FPVs. The mean φ calculated between April and August for all the FPV array configuration scenarios ranged between 9.42 J/m^3 and 9.73 J/m^3, reflecting little effect of either the small changes to surface coverage or the light islands on the lake's thermal structure.

4. Discussion

4.1. Water body thermal responses to FPVs

FPV impacts on thermal response may arise through different mechanisms given the reduced solar radiation (decreases thermal stratification) and sheltering of wind speed (increases thermal stratification given limited advective and convective heat transfer to the deeper layers) (MacIntyre and Hamilton, 2024). Therefore, reducing both solar radiation and wind speed is expected to have a stronger effect on the hypolimnetic region's temperature compared to the surface, as evidenced by our model results. The main difference among the scenarios investigated for thermal stratification are observed between model results for the simulation without FPVs and those that include the panels. Thus, the range of changes to incoming solar radiation and wind speed with FPV design had little to no effect on the mixing patterns in this study. Overall, results for thermal stratification indicate that wind sheltering impacts on mixing patterns prevailed compared to shading from solar radiation, resulting in stronger stratification for the FPVs simulation. This is explained by the lack of surface inflows or outflows to the system, making the wind the water body's main mixing energy source.

Our simulations were consistent with the expected water column cooling effect due to FPVs, in temperate regions, as simulated by Exley et al. (2021) when modelling the south basin of Windermere, a lake in England (maximum depth of 42 m and surface area of 6.7 km^2), Exley et al. (2025) in a drinking water reservoir in England (mean depth of 15 m, surface area of 1.28 km^2), and by Ilgen et al. (2023) in an artificial dredged lake in Germany (mean depth 24 m, maximum depth 70 m, surface area 0.37 km^2). These systems (Exley et al., 2021, 2025; Ilgen et al., 2023) differ in morphology, hydrological connectivity, and local meteorological forcing, yet all are in temperate climates and show consistent cooling responses, suggesting that this effect represents a first-order impact under comparable climatic conditions rather than a site-specific outcome. Further, our results show vertical differences in

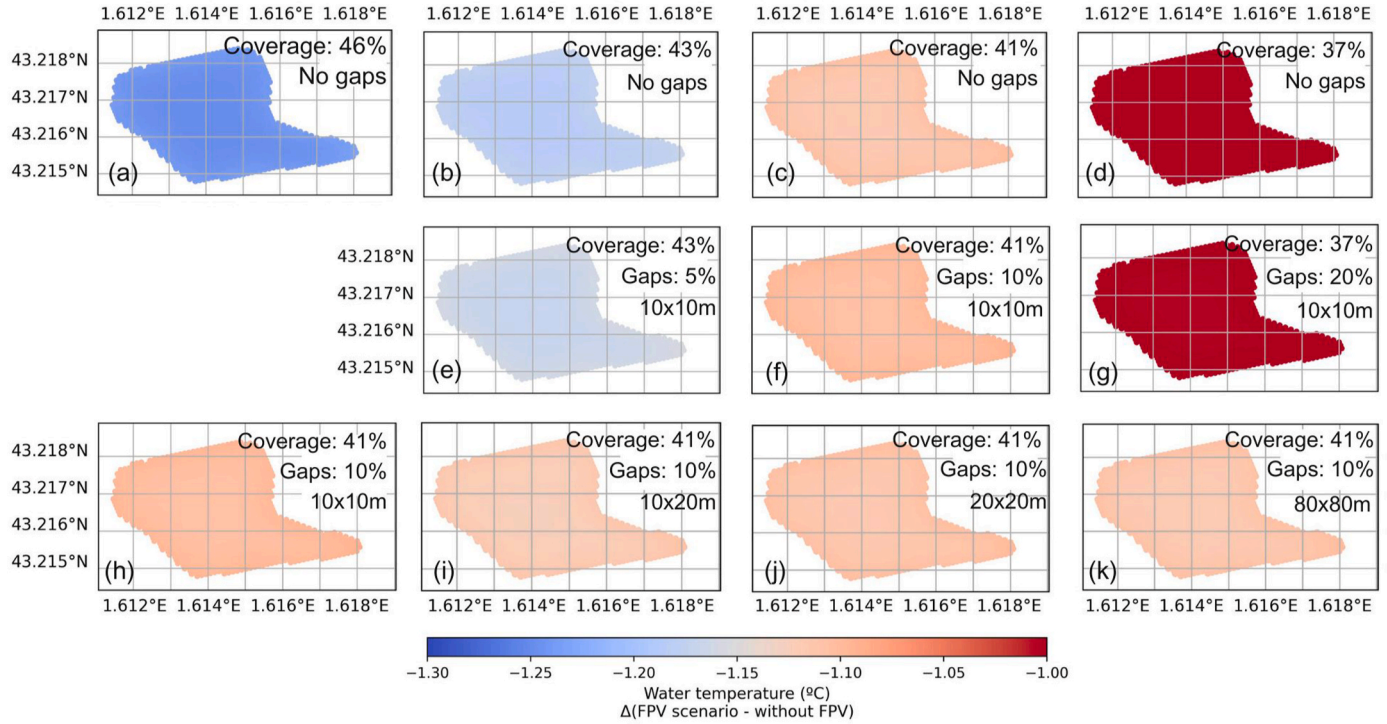

Fig. 4. Model output for surface water temperature at the day and time with the largest temperature difference comparing simulations with and without FPVs (August 7, 2023 at 6 a.m.).

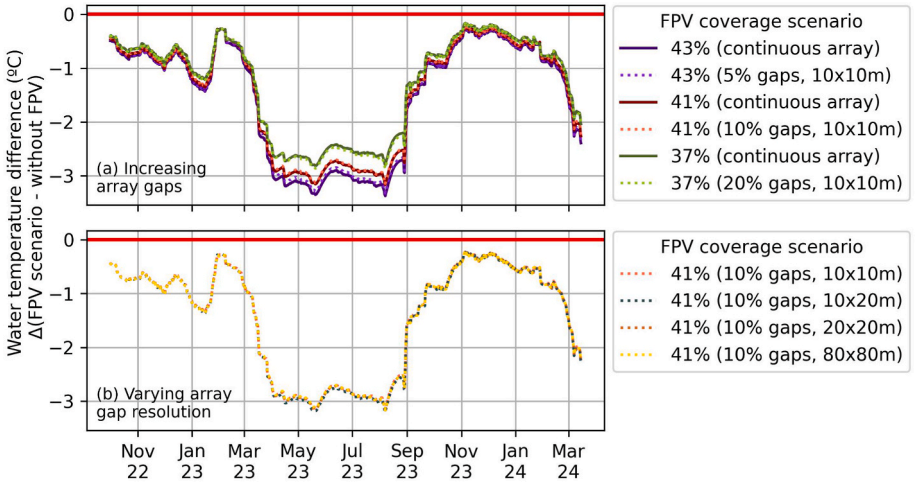

Fig. 5. Modelled water temperature deviation for multiple “light islands” scenarios in the FPVs array, horizontally averaged for cells with FPVs.

FPV impacts that are consistent with a field based study of a drinking water reservoir (maximum depth of 17 m) by Prandini et al. (2025), which reported intensified cooling effects from the FPVs with depth. In contrast, however, Exley et al. (2021) and Ilgen et al. (2023) reported deep water temperatures to decrease less than surface waters. These variations among studies are expected as thermal profile and stratification responses are complex emergent effects that are likely to differ among water bodies, especially in different climate zones, as a result of among-site variability in incoming solar radiation, cloudiness, catchment topography, wind direction and fetch.

Our simulations recreated the seasonality of FPV impacts that has been reported previously, with larger cooling effects reported over warmer months (Nobre et al., 2025) and provided further mechanistic insights into such variability. Our results provide evidence that, at the start of spring, the effects of solar radiation reduction are stronger than those of wind speed reduction, as the surface layer showed a larger temperature decrease compared to the deeper layers. As air temperature progressively increased into the summer, the deeper layers experienced a larger temperature decrease compared to the surface layers, displaying the effects of reduced wind-induced advective transport. Moreover, considering FPV impacts upon thermal stratification and water column stability, our results indicate that wind sheltering impacts on mixing patterns prevailed compared to shading from solar radiation, resulting in stronger stratification for the FPVs simulation. This is in agreement with reports by Bredeweg et al. (2025) in one of the reservoirs simulated using a 2D model, and Ilgen et al. (2023) in simulations using a 3D model approach for coverages up to 30%. Contrastingly, Exley et al. (2021) reported weaker thermal stratification under the majority of the FPV scenarios tested using a 1D model, and Bredeweg et al. (2025) reported limited change to thermal stratification for many reservoirs

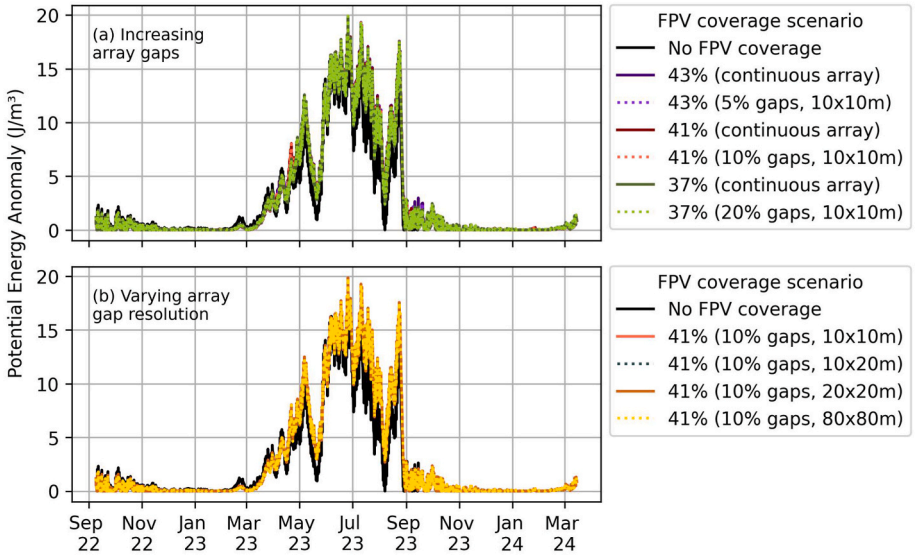

Fig. 6. Modelled Potential Energy Anomaly (φ) for multiple "light islands" scenarios in the FPVs array, maximum φ calculated for cells with FPVs.

regardless of FPV extent.

Existing evidence suggests cooler water temperatures under FPV arrays (Liu et al., 2023; Nobre et al., 2025), which could offset increased air temperatures due to climate change as simulated by Exley et al. (2025). However, our results underscore the importance of understanding the meteorological and physical mechanisms that would underpin such an effect. In particular, the role of reduced wind speed and mixing processes (and not only reduced light penetration) is of key importance as this could result in stronger stratification; an effect not always taken into account. Moreover, recent findings in tropical and subtropical locations report increased water temperature due to FPV deployment (Prandini et al., 2025; Yang et al., 2022), potentially enhancing global warming effects. Climate change is already affecting the multiple meteorological processes driving lake physics and ecology (e.g. wind speed and direction, rainfall, relative humidity) in complex ways (Tong et al., 2023; Woolway et al., 2020). The non-linear relationships among these changes pose challenges to predicting impacts, which highlights the importance of understanding local dynamics and taking them into account prior to deploying FPVs.

4.2. *Spatiotemporal impacts of light island design*

Upon testing multiple FPV array scenarios, we found that water temperatures were cooler when FPVs were present than when they were absent, and that there was limited spatial variability in this effect, i.e., the effect of the array was noted in areas not covered by the arrays as well as areas under them. Similarly, Nobre et al. (2025), in a BACI study of gravel pit lakes in the same region, found an FPVs-induced decrease in water temperature in open water locations that were adjacent to, and not covered by, the array. In contrast, Prandini et al. (2025) found small but consistently higher water temperatures at the FPV's location when investigating a larger reservoir (8.7 km^2 of surface area compared to $<$0.20 km^2 in this study and that of Nobre et al. (2025) with less than 1 % of its surface covered. Similarly, Liu et al. (2023) reported significant spatial differences in water temperature between FPV-covered and open water locations, when evaluating mining reservoirs with 45 % and 8 % surface coverages. Importantly, these studies (Liu et al., 2023; Prandini et al., 2025) considered open water locations within the same water body, but beyond the extent of deployed FPV arrays, as control locations. Given horizontal circulation and heat transport processes within large water bodies, a certain degree of spatial autocorrelation can be expected for conditions across the open water zone, and the strength of this influence will depend on the distance between the FPVs array and the control (uncovered) areas that are studied.

The magnitude of water body impacts of FPV arrays is known to be dependent on the surface coverage (Exley et al., 2022; Ilgen et al., 2023; Yang et al., 2022). Here, the difference in temperature impacts among the scenarios, even with a modest difference in FPV coverages - approximately 5% - indicated that inclusion of light islands has minimal effect. The similarity in model predictions is attributable to horizontal momentum transfer from mixing patterns and heat transport, which was noted to influence the FPV's impacts more than the reduced solar radiation. Moreover, the spatially homogeneous effect of the array across the whole surface of the lake (i.e. the same water temperature reduction observed both under the array and in open water) is consistent with the lack of spatially heterogeneous light islands impacts beneath the array itself.

In contrast to the predicted insensitivity of water temperature and stability to these light island configurations, we would nevertheless expect such designs to impact several water quality and ecological states. For example, phytoplankton growth, composition, and biomass could still be impacted by such design decisions through design-dependent impacts on underwater light regime, even if temperatures are less affected. Impacts on phytoplankton would be expected to cascade to biogeochemical cycles and food web processes. Li et al. (2023) and Nobre et al. (2025) when analysing, respectively, rotifer communities and diatom assemblages, found different species composition under the FPVs compared to open water, despite lower phytoplankton biomass (Li et al., 2023). Therefore, increasing light availability in the water column under the arrays is a potential tool to mitigate shading impacts of large-scale arrays, and may yet prove to be an effective tool in minimizing effects on local biodiversity. Existing evidence of lake-specific responses to FPV arrays (Liu et al., 2024; Nobre et al., 2023), underscores the importance of investigating techniques, such as the implementation of light islands to minimize the FPVs' effects, more widely.

5. Conclusions

This study advances knowledge of how the thermal structure of a lake responds to FPV coverage and multiple array configuration designs through 3D computational modelling. Our findings showed that FPVs alter the thermal regime by reducing both solar radiation and wind speed, with effects that vary seasonally and by depth. Wind sheltering effects dominated over shading during warmer months, leading to stronger stratification, although responses are likely to be system-

specific and sensitive to model dimensionality. Spatial analyses revealed that FPVs can alter water temperature both under and beyond the array, but the spatial extent of effects depends on lake size, FPV coverage, and circulation. Even small changes in surface coverage (~5%) had large effects on water temperature responses. Variations to light islands had a limited impact on thermal stratification but may reduce ecological disruptions by enhancing underwater light availability.

In conclusion, to enable generalisation of findings across different water bodies and FPV configurations, three critical areas for future research are highlighted: (i) field campaigns including BACI designs, (ii) understanding the implications of model dimensionality on FPV representation, and (iii) more holistic investigation of the impacts of different configurations of FPV arrays (e.g. a wider range of light island geometries). Future research should combine FPV design scenarios with empirical before and after deployment measurements to evaluate responses in water quality, thermal stratification and ecological dynamics (e.g. primary production, biodiversity components). Advancing our understanding of how model dimensionality and the limitations associated with applying single attenuation factors to meteorological forcing influence predicted lake responses will enhance confidence in simulation-based predictions. Moreover, multidimensional models remain key to investigating localised effects, including how different FPV configurations, expanding on the scenarios applied to this study in both array design and location at the water surface, alter how they relate to ecological changes. These complex interactions among water bodies' morphology, hydrodynamic processes and ecological functioning drive varying responses to FPVs. Therefore, integrating FPV deployment strategies with computational modelling brings the opportunity to balance energy production with sustainable decisions, ultimately strengthening FPVs' contribution to climate change mitigation.

CRediT authorship contribution statement

Sofia M.G. Rocha: Writing – original draft, Visualization, Validation, Software, Project administration, Methodology, Formal analysis, Data curation, Conceptualization. **Regina L.G. Nobre:** Writing – review & editing, Visualization, Validation, Resources, Investigation, Formal analysis. **Diego A. Casas:** Writing – review & editing, Validation, Software, Formal analysis, Data curation. **Stephen J. Thackeray:** Writing – review & editing, Visualization, Supervision, Resources, Project administration, Methodology, Funding acquisition, Conceptualization. **Alona Armstrong:** Writing – review & editing, Visualization, Supervision, Resources, Project administration, Methodology, Funding acquisition, Conceptualization. **Stéphanie Boulêtreau:** Writing – review & editing, Resources. **Julien Cucherousset:** Writing – review & editing, Resources, Funding acquisition, Conceptualization. **Andrew Folkard:** Writing – review & editing, Visualization, Supervision, Resources, Project administration, Methodology, Funding acquisition, Conceptualization.

Funding

Sofia M. G. Rocha was supported by the Engineering and Physical Sciences Research Council (EPSRC) via a Doctoral Training Programme [grant number EP/W524438/1]. Regina Nobre was funded by the European Union's Horizon 2020 research and Innovation programme under the Marie Skłodowska-Curie grant agreement no 101,065,785 (ECLIPSE project). This work is part of the long-term Studies in Ecology and Evolution (SEE-Life) program of the CNRS and was supported by ADEME (SOLAKE project) and OFB (FLOATIX project).

Declaration of competing interest

The authors declare that they have no known competing financial interests or personal relationships that could have appeared to influence the work reported in this paper.

Acknowledgements

We are grateful to CNR for providing access to the lake and meteorological data. The authors acknowledge the use of High-End Computing (HEC) cluster resources provided by Lancaster University. We thank the HEC support staff for their assistance and recognize that access to these resources was essential for completing the large-scale simulations and data analyses presented in this study.

Appendix A. Supplementary data

Supplementary data to this article can be found online at https://doi.org/10.1016/j.jenvman.2026.129415.

Data availability

Data will be made available on request.

References

Almeida, R.M., Schmitt, R., Grodsky, S.M., Flecker, A.S., Gomes, C.P., Zhao, L., Liu, H., Barros, N., Kelman, R., McIntyre, P.B., 2022. Floating solar power could help fight climate change — let's get it right. Nature 606, 246–249. https://doi.org/10.1038/d41586-022-01525-1.

Al-Widyan, M., Khasawneh, M., Abu-Dalo, M., 2021. Potential of floating photovoltaic technology and their effects on energy output, water quality and supply in Jordan. Energies 14, 8417. https://doi.org/10.3390/en14248417.

Amadori, M., Giovannini, L., Toffolon, M., Piccolroaz, S., Zardi, D., Bresciani, M., Giardino, C., Luciani, G., Kliphuis, M., van Haren, H., Dijkstra, H.A., 2021. Multi-scale evaluation of a 3D lake model forced by an atmospheric model against standard monitoring data. Environ. Model. Software 139, 105017. https://doi.org/10.1016/j.envsoft.2021.105017.

Armstrong, A., Page, T., Thackeray, S.J., Hernandez, R.R., Jones, I.D., 2020. Integrating environmental understanding into freshwater floatovoltaic deployment using an effects hierarchy and decision trees. Environ. Res. Lett. 15, 114055. https://doi.org/10.1088/1748-9326/abbf7b.

Bredeweg, E.M., Arismendi, I., Murphy, C.A., Henkel, S.K., 2025. Modeling diverse environmental responses of reservoirs to floating photovoltaic systems. Limnologica, 126293. https://doi.org/10.1016/j.limno.2025.126293.

Brown, J.H., Gillooly, J.F., Allen, A.P., Savage, V.M., West, G.B., 2004. Toward a metabolic theory of ecology. Ecology 85, 1771–1789. https://doi.org/10.1890/03-9000.

Deltares, 2020. User manual Delft3D-Flow. Technical Report. Deltares, Delft, The Netherlands.

DNV, 2024. Energy transition outlook 2024. https://www.dnv.com/energy-transition-outlook.

Dörenkämper, M., Wahed, A., Kumar, A., De Jong, M., Kroon, J., Reindl, T., 2021. The cooling effect of floating PV in two different climate zones: a comparison of field test data from the Netherlands and Singapore. Sol. Energy 219, 15–23. https://doi.org/10.1016/j.solener.2021.03.051.

El Hammoumi, A., Chalh, A., Allouhi, A., Motahhir, S., El Ghzizal, A., Derouich, A., 2021. Design and construction of a test bench to investigate the potential of floating PV systems. J. Clean. Prod. 278, 123917. https://doi.org/10.1016/j.jclepro.2020.123917.

Exley, G., Armstrong, A., Page, T., Jones, I.D., 2021. Floating photovoltaics could mitigate climate change impacts on water body temperature and stratification. Sol. Energy 219, 24–33. https://doi.org/10.1016/j.solener.2021.01.076.

Exley, G., Page, T., Thackeray, S.J., Folkard, A.M., Couture, R.-M., Hernandez, R.R., Cagle, A.E., Salk, K.R., Clous, L., Whittaker, P., Chipps, M., Armstrong, A., 2022. Floating solar panels on reservoirs impact phytoplankton populations: a modelling experiment. J. Environ. Manag. 324, 116410. https://doi.org/10.1016/j.jenvman.2022.116410.

Exley, G., Page, T., Olsson, F., Thackeray, S.J., Chipps, M.J., Armstrong, A., Folkard, A. M., 2025. Modelling of the potential of floating photovoltaics for mitigating climate change impacts on reservoirs. Knowl. Manag. Aquat. Ecosyst. 26. https://doi.org/10.1051/kmae/2025021.

Gimenez, M., Villéger, S., Grenouillet, G., Cucherousset, J., 2023. Stocking practices shape the taxonomic and functional diversity of fish communities in gravel pit lakes. Fish. Manag. Ecol. 30, 603–614. https://doi.org/10.1111/fme.12621.

Guo, S., Zhu, D., Chen, Y., 2023. Modelling and analyzing a unique phenomenon of surface water temperature rise in a tropical, large, riverine reservoir. Water Resour. Manag. 37, 1711–1727. https://doi.org/10.1007/s11269-023-03450-y.

Hosseini-Sadabadi, S.A., Rousseau, A.N., Laurion, I., Behmel, S., Sadeghian, A., Foulon, E., Wauthy, M., Cantin, A.-M., 2024. Spatiotemporal insights of phytoplankton dynamics in a northern, rural-urban lake using a 3D water quality model. J. Environ. Manag. 370, 122687. https://doi.org/10.1016/j.jenvman.2024.122687.

Ilgen, K., Goulart, C.B., Hilgert, S., Schindler, D., Weyer, K. van de, Bueno, R. de C., Bleninger, T., Lastrico, R., Gfüllner, L., Graef, A., Fuchs, S., Lange, J., 2025. Hydrological and ecological effects of floating photovoltaic systems: a model

comparison considering mussel, periphyton, and macrophyte growth. Knowl. Manag. Aquat. Ecosyst. 11. https://doi.org/10.1051/kmae/2025008.
Ilgen, K., Schindler, D., Wieland, S., Lange, J., 2023. The impact of floating photovoltaic power plants on lake water temperature and stratification. Sci. Rep. 13, 7932. https://doi.org/10.1038/s41598-023-34751-2.
Ishikawa, M., Gonzalez, W., Golyjeswski, O., Sales, G., Rigotti, J.A., Bleninger, T., Mannich, M., Lorke, A., 2022. Effects of dimensionality on the performance of hydrodynamic models for stratified lakes and reservoirs. Geosci. Model Dev. (GMD) 15, 2197–2220. https://doi.org/10.5194/gmd-15-2197-2022.
Ji, Q., Li, K., Wang, Y., Feng, J., Li, R., Liang, R., 2022. Effect of floating photovoltaic system on water temperature of deep reservoir and assessment of its potential benefits, a case on Xiangjiaba Reservoir with hydropower station. Renew. Energy 195, 946–956. https://doi.org/10.1016/j.renene.2022.06.096.
Kumar, M., Kumar, A., 2020. Experimental characterization of the performance of different photovoltaic technologies on water bodies. Prog. Photovoltaics Res. Appl. 28, 25–48. https://doi.org/10.1002/pip.3204.
Li, P., Gao, X., Jiang, J., Yang, L., Li, Y., 2020. Characteristic analysis of water quality variation and fish impact study of fish-lighting complementary photovoltaic power station. Energies 13, 4822. https://doi.org/10.3390/en13184822.
Li, W., Wang, Y., Wang, G., Liang, Y., Li, C., Svenning, J.-C., 2023. How do rotifer communities respond to floating photovoltaic systems in the subsidence wetlands created by underground coal mining in China? J. Environ. Manag. 339, 117816. https://doi.org/10.1016/j.jenvman.2023.117816.
Lima Neto, I.E., 2025. Two-dimensional modeling of the impact of surface coverage on the evaporation and hydrodynamics of a shallow tropical reservoir. J. Hydrol., 134217 https://doi.org/10.1016/j.jhydrol.2025.134217.
Liu, Z., Ma, C., Li, X., Deng, Z., Tian, Z., 2023. Aquatic environment impacts of floating photovoltaic and implications for climate change challenges. J. Environ. Manag. 346, 118851. https://doi.org/10.1016/j.jenvman.2023.118851.
Liu, Z., Ma, C., Yang, Y., Li, X., Gou, H., Folkard, A.M., 2024. Water temperature and energy balance of floating photovoltaic construction water area—field study and modelling. J. Environ. Manag. 365, 121494. https://doi.org/10.1016/j.jenvman.2024.121494.
MacIntyre, S., Hamilton, D.P., 2024. Chapter 7 - fate of heat. In: Jones, I.D., Smol, J.P. (Eds.), Wetzel's Limnology, fourth ed. Academic Press, San Diego, pp. 95–153. https://doi.org/10.1016/B978-0-12-822701-5.00007-0.
Majumder, A., Innamorati, R., Frattolillo, A., Kumar, A., Gatto, G., 2021. Performance analysis of a floating photovoltaic System and estimation of the evaporation losses reduction. Energies 14, 8336. https://doi.org/10.3390/en14248336.
Nisar, H., Kashif Janjua, A., Hafeez, H., Shakir, S., Shahzad, N., Waqas, A., 2022. Thermal and electrical performance of solar floating PV system compared to on-ground PV system-an experimental investigation. Sol. Energy 241, 231–247. https://doi.org/10.1016/j.solener.2022.05.062.
Nobre, R., Boulêtreau, S., Colas, F., Azemar, F., Tudesque, L., Parthuisot, N., Favriou, P., Cucherousset, J., 2023. Potential ecological impacts of floating photovoltaics on lake biodiversity and ecosystem functioning. Renew. Sustain. Energy Rev. 188, 113852. https://doi.org/10.1016/j.rser.2023.113852.
Nobre, R., Rocha, S.M., Healing, S., Ji, Q., Boulêtreau, S., Armstrong, A., Cucherousset, J., 2024. A global study of freshwater coverage by floating photovoltaics. Sol. Energy 267, 112244. https://doi.org/10.1016/j.solener.2023.112244.
Nobre, R.L.G., Vagnon, C., Boulêtreau, S., Colas, F., Azémar, F., Tudesque, L., Parthuisot, N., Millet, P., Cucherousset, J., 2025. Floating photovoltaics strongly reduce water temperature: a whole-lake experiment. J. Environ. Manag. 375, 124230. https://doi.org/10.1016/j.jenvman.2025.124230.
Piccioni, F., Casenave, C., Lemaire, B.J., Le Moigne, P., Dubois, P., Vinçon-Leite, B., 2021. The thermal response of small and shallow lakes to climate change: new insights from 3D hindcast modelling. Earth Syst. Dynam. 12, 439–456. https://doi.org/10.5194/esd-12-439-2021.
Python Software Foundation, 2023. v.3.11.04 [software], Version 3.11.04. https://www.python.org/.
Prandini, M.K., Bueno, R. de C., Rigotti, J.A., Bleninger, T., Mannich, M., Novak, L.H., 2025. High frequency monitoring for impact assessment of temperature, oxygen and radiation in floating photovoltaic system. Sci. Rep. 15, 19719. https://doi.org/10.1038/s41598-025-96257-3.
Ramanan, C.J., Lim, K.H., Kurnia, J.C., Roy, S., Bora, B.J., Medhi, B.J., 2024. Towards sustainable power generation: recent advancements in floating photovoltaic technologies. Renew. Sustain. Energy Rev. 194, 114322. https://doi.org/10.1016/j.rser.2024.114322.
Rocha, S.M.G., Armstrong, A., Thackeray, S.J., Hernandez, R.R., M Folkard, A., 2024. Environmental impacts of floating solar panels on freshwater systems and their techno-ecological synergies. Environ. Res. Infrastruct. Sustain. 4, 042002. https://doi.org/10.1088/2634-4505/ad8e81.
Rocha, S.M.G., Molinas, E., Rodrigues, I.S., Lima Neto, I.E., 2023. Assessment of total evaporation rates and its surface distribution by tridimensional modelling and remote sensing. J. Environ. Manag. 327, 116846. https://doi.org/10.1016/j.jenvman.2022.116846.
Rueda, F.J., Ramón, C.L., Schladow, S.G., 2025. The hydrodynamic, thermodynamic, and mixing impacts of floating photovoltaics on the surface of a Lake. Water Resour. Res. 61. https://doi.org/10.1029/2025WR039917 e2025WR039917.
Sacramento, E.M.D., Carvalho, P.C.M., Araújo, J.C., Riffel, D.B., Corrêa, R.M.D.C., Pinheiro Neto, J.S., 2015. Scenarios for use of floating photovoltaic plants in Brazilian reservoirs. IET Renew. Power Gener. 9, 1019–1024. https://doi.org/10.1049/iet-rpg.2015.0120.
Santafé, M.R., Ferrer Gisbert, P.S., Sánchez Romero, F.J., Torregrosa Soler, J.B., Ferrán Gozálvez, J.J., Ferrer Gisbert, C.M., 2014. Implementation of a photovoltaic floating cover for irrigation reservoirs. J. Clean. Prod. 66, 568–570. https://doi.org/10.1016/j.jclepro.2013.11.006.
Schallenberg, M., de Winton, M.D., Verburg, P., Kelly, D.J., Hamill, K.D., Hamilton, D.P., 2013. Ecosystem services of lakes. Ecosystem Services in New Zealand - Conditions and Trends, pp. 203–225.
Tong, Y., Feng, L., Wang, X., Pi, X., Xu, W., Woolway, R.I., 2023. Global lakes are warming slower than surface air temperature due to accelerated evaporation. Nat. Water 1, 929–940. https://doi.org/10.1038/s44221-023-00148-8.
Woolway, R.I., Kraemer, B.M., Lenters, J.D., Merchant, C.J., O'Reilly, C.M., Sharma, S., 2020. Global lake responses to climate change. Nat. Rev. Earth Environ. 1, 388–403. https://doi.org/10.1038/s43017-020-0067-5.
Woolway, R.I., Zhao, G., Rocha, S.M.G., Thackeray, S.J., Armstrong, A., 2024. Decarbonization potential of floating solar photovoltaics on lakes worldwide. Nat. Water 2, 566–576. https://doi.org/10.1038/s44221-024-00251-4.
Xia, Z., Li, Y., Guo, S., Chen, R., Zhang, W., Zhang, P., Du, P., 2023. Mapping global water-surface photovoltaics with satellite images. Renew. Sustain. Energy Rev. 187, 113760. https://doi.org/10.1016/j.rser.2023.113760.
Xu, C., Zhang, J., Bi, X., Xu, Z., He, Y., Gin, K.Y.-H., 2017. Developing an integrated 3D-hydrodynamic and emerging contaminant model for assessing water quality in a Yangtze Estuary reservoir. Chemosphere 188, 218–230. https://doi.org/10.1016/j.chemosphere.2017.08.121.
Xu, J., Pan, J., Devlin, A.T., 2023. Variations in chlorophyll-a concentration in response to hydrodynamics in a flow-through lake: remote sensing and modeling studies. Ecol. Indic. 148, 110128. https://doi.org/10.1016/j.ecolind.2023.110128.
Yang, P., Chua, L.H.C., Irvine, K.N., Nguyen, M.T., Low, E.-W., 2022. Impacts of a floating photovoltaic system on temperature and water quality in a shallow tropical reservoir. Limnology 23, 441–454. https://doi.org/10.1007/s10201-022-00698-y.
Zhao, T., Grenouillet, G., Pool, T., Tudesque, L., Cucherousset, J., 2016. Environmental determinants of fish community structure in gravel pit lakes. Ecol. Freshw. Fish 25, 412–421. https://doi.org/10.1111/eff.12222.
Zheng, X.-N., Wu, D.-X., Huang, C.-Q., Wu, Q.-Y., Guan, Y.-T., 2022. Impacts of hydraulic retention time and inflow water quality on algal growth in a shallow lake supplied with reclaimed water. Water Cycle 3, 71–78. https://doi.org/10.1016/j.watcyc.2022.04.004.